Image Anal Stereol 2026;45:95-101
Original Research Paper doi: 10.5566/ias.4005

STEREOLOGY FOR THE WEIBEL-PALADE BODIES

LUIS M. CRUZ-ORIVE

University of Cantabria, (Ret.), E-39005 Santander, Spain
e-mail: luis.cruz@unican.es
(Received May 5, 2026; revised June 15, 2026; accepted June 16, 2026)

ABSTRACT

Weibel-Palade (WP) bodies are often rod shaped endothelial cell organelles playing a role in blood coagulation processes. In 1962, E.R. Weibel first observed a longitudinal transect of one such organelle in an electron micrograph, measuring about $0.06\,\mu\text{m} \times 1.0\,\mu\text{m}$. He noticed that the a priori probability of such an event - analogous to that of hitting both ends of a rod by a random plane - should be "extremely low". The main purpose of this note is to make an educated guess of that probability - more precisely, the expected proportion of transects affecting both bases of a finite right circular cylinder, among all possible isotropic and uniform random (IUR) slabs, or planes, hitting the cylinder.

Keywords: Hitting probabilities, motion invariant hitting measure, plane probe, right circular cylinder, rod, slab probe.

In memory of Ewald Rudolf Weibel (1929-2019).

INTRODUCTION

The main motivation of this note stems from the following extract from Weibel (2012b):

> *It was on 14 February 1962 ... that I came upon the cross-section of a small pulmonary artery while scanning the section of a rat lung ... I took a low-power electronmicrograph out of curiosity, even though the section was scratched and a bit dirty, with stain smudges and a long 'dust' particle ... However, when I studied the prints it became evident that what had appeared as dust was not dust at all, but rather something biological: a long and slim rod-shaped body contained in the cytoplasm, which had been fortuitously or perhaps miraculously cut longitudinally in this micrograph. The probability of cutting a rod 20 times as long as thick along its axis from one end to the other is extremely low; random sections would have to hit the rod mostly cross-wise or obliquely at various angles, generating round or elliptic profiles, depending on the section angle.*

Decades later, it was discovered that such organelles - known as 'Weibel-Palade bodies' (Weibel and Palade, 1964) - contain the so-called 'von Willebrand factor', which is a blood glycoprotein involved in coagulation processes. For details see Weibel (2012a, b). See also Note 3.

Our main purpose is to provide some theoretical support to Weibel's assertions. Modern stereology does not advocate particle shape models; exceptionally, however, the right circular cylinder is a reasonable shape model for Weibel-Palade bodies resembling rods (Fig. 1).

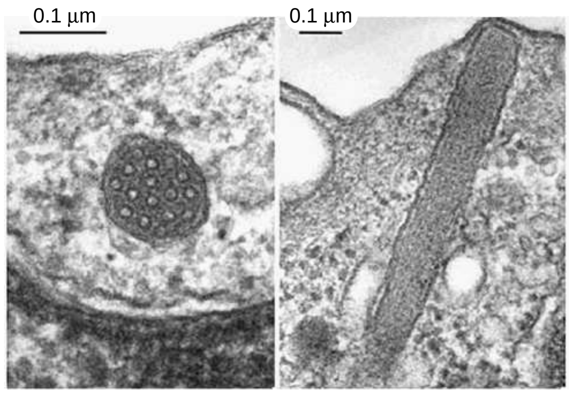

Fig. 1: *Approximately transversal and longitudinal TEM transects, each of a Weibel-Palade body, tentatively suggesting a right circular cylinder model to compute hitting probabilities. Courtesy of E.R. Weibel, also published in Weibel (2012b).*

The numerical results will be only orientative, not unbiased estimates. With the rod assumption, in the following section the following results are obtained:

- Conditional probability P_k that a slab probe of known thickness hitting a bounded right circular cylinder isotropically and uniformly at random, (IUR, e.g. Miles and Davy, 1976), hits k bases of the cylinder ($k = 0, 1, 2$), (Proposition 1). Thus, P_2 predicts the proportion of 'longitudinal' transects among all possible IUR cylinder transects.
- Conditional probability that the slab probe contains

the axis (or 'spine') of the cylinder (Corollary 1).

- Expressions of P_k when the probe is a plane (Corollary 2). This case may be realistic inasmuch as a transmission electron microscopical (TEM) section (which may be regarded as an ultrathin slab section) is often stained mainly on its upper face.

Tentative numerical results are given for a cylinder 1.00 μm long and 0.07 μm in diameter. (The WP body transect marked with the two red arrows in Fig. 2 measures about $0.06\,\mu\text{m} \times 1.00\,\mu\text{m}$). The problem of estimating WP body number and volume is briefly discussed in the last section.

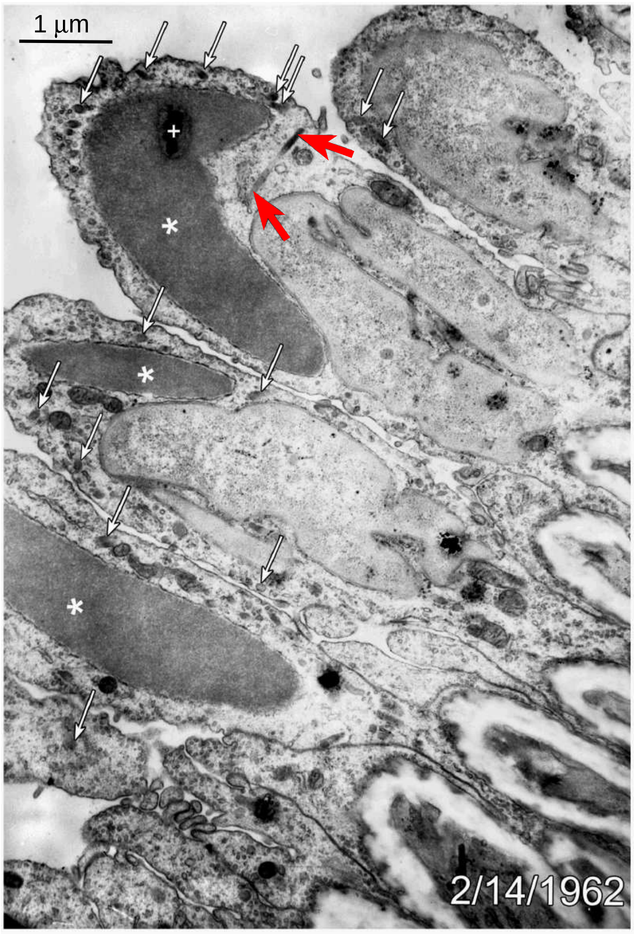

Fig. 2: *Original electron micrograph in which E.R. Weibel identified a longitudinal transect of a WP body for the first time (larger arrows, coloured in red for this note). Most WP body transects are nearly elliptical; a number of them were marked with white arrows by E.R. Weibel himself, who suggested that there should be "almost twice as many" in the image (personal communication, 2013). Courtesy of E.R. Weibel, also published in Weibel (2012b).*

The approach used here is design based, but the results apply also to the model based case (for a brief explanation see Cruz-Orive, 2017, p. 153) without change.

HITTING PROBABILITIES INVOLVING A SLAB AND A RIGHT CIRCULAR CYLINDER

PRELIMINARIES

A reasonable model for a class of WP bodies is a solid and bounded right circular cylinder $K \subset \mathbb{R}^3$, see Fig. 3a. Each of the two bases of K is a circular disk of radius r, and its height has a finite length $2h$, (the factor "2" will simplify the notation). Adopt an orthogonal reference trihedron $Ox_1x_2x_3$ with origin O at the centre of K, and the Ox_3 axis along the axis of symmetry of K. In Cartesian coordinates,

$$K := \left\{x \in \mathbb{R}^3 : x_1^2 + x_2^2 \leq r^2, -h \leq x_3 \leq h\right\}, \qquad (1)$$

where $x := (x_1, x_2, x_3)$. Hereafter, "$A := B$" means "A is defined by B", or "B is denoted by A".

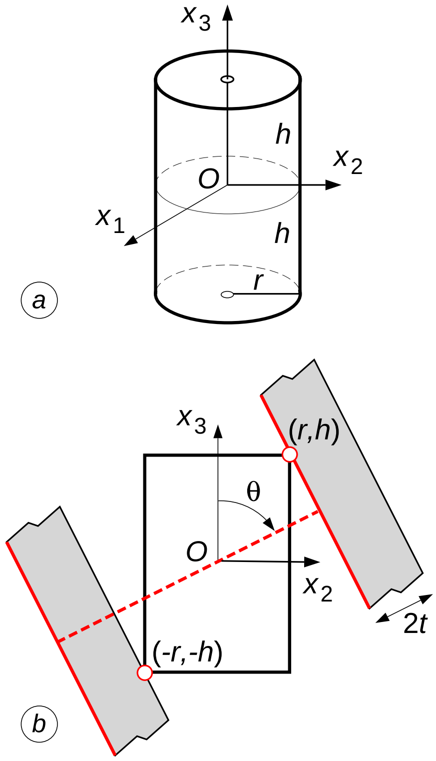

Fig. 3: *(a) Cylinder model, see Eq. 1. (b) Detail of the derivation of Eq. 10. The broken line represents the range of the slab hitting the cylinder for a given colatitude θ of the normal to the slab.*

- A plane is defined as

$$L(p,u) := \left\{x \in \mathbb{R}^3 : \sum_{i=1}^{3} x_i u_i = p\right\}, \qquad (2)$$

where $u := (u_1, u_2, u_3)$ are the direction cosines of an axis normal to the plane, whereas p is the signed distance of the plane from O. If the plane contains a fixed point $x_0 := (x_{01}, x_{02}, x_{03})$, then,

$$p := p\,(x_0, u) = \sum_{i=1}^{3} x_{0i} u_i \qquad (3)$$

- In spherical polar coordinates,

$$u := (\sin\theta\cos\phi, \sin\theta\sin\phi, \cos\theta) \qquad (4)$$

  where $\phi \in [0, 2\pi)$ is the longitude angle, with origin at Ox_1, and $\theta \in [0, \pi/2]$ is the colatitude, with origin at the polar axis Ox_3.

- A slab $L_t := L_t(p, u) \subset \mathbb{R}^3$ of thickness $2t$ is the portion of space between two parallel planes a distance $2t$ apart, namely $L(p, u)$, which is adopted as the reference face, and $L(p + 2t, u)$, (Santaló, 1936; Cruz-Orive, 2024, Fig. 1.2.5b).

Define the events,

$$E_k := {}''L_t \text{ hits } k \text{ bases of } K'', \ (k = 0, 1, 2). \qquad (5)$$

The problem is to find the conditional probabilities

$$P_k(h, r, t) := \mathbb{P}\left(E_k \mid L_t \cap K \neq \emptyset\right). \qquad (6)$$

In the present context it is convenient to express the preceding probabilities as ratios of motion invariant measures. Thus,

$$P_k(h, r, t) = \frac{\mu_k(h, r, t)}{\mu(h, r, t)} := \frac{\mu_k}{\mu}, \qquad (7)$$

where μ_k and μ denote the measures of the slabs hitting exactly k bases of K, and hitting K, respectively. Each measure is given by a triple integral, with respect to $\{\phi, \theta, p\}$, of a known integrand depending on $\{h, r, t, \phi, \theta, p\}$. To warrant independence from the choice of the reference frame, the integral is with respect to the motion invariant density of the slab L_t, which is the same as the one of the reference face, namely,

$$\mathrm{d}L_t(p, \phi, \theta) = \sin\theta\,\mathrm{d}\phi\,\mathrm{d}\theta\,\mathrm{d}p \qquad (8)$$

The procedure is illustrated first by computing $\mu := \mu(h, r, t)$. The cylinder K is invariant with respect to rotations about the polar axis Ox_3, hence, for any value of ϕ the measure of slabs hitting K does not depend on ϕ. Thus, to compute the latter measure it suffices to set $\phi = \pi/2$ and $x_1 = 0$, say, whereby K is replaced with the rectangle $[-r, r] \times [-h, h]$ in the plane Ox_2x_3, (Fig. 3b), whereas the trace of the reference face of the slab in that plane is a straight line $L(p, \theta)$, (coloured in red in Figs. 3b and 4), where

$$p := p\,(x_{02}, x_{03}, \theta) = x_{02}\sin\theta + x_{03}\cos\theta, \qquad (9)$$

which is equivalent to Eq. 3 with $\phi = \pi/2$. In Figs. 3b and 4, the slab L_t is normal to the plane of the paper, and its trace is a stripe of thickness $2t$.

With reference to Fig. 3b, for any $\theta \in [0, \pi/2]$, the event $L_t \cap K \neq \emptyset$ holds whenever the face $L(p + t, \theta)$ of the slab first meets the corner point $(-r, -h)$, and the entire stripe moves parallel to itself until the reference face $L(p, \theta)$ meets the corner point (r, h). Now, using the density in Eq. 8,

$$\begin{aligned}\mu &= \int_0^{2\pi} \mathrm{d}\phi \int_0^{\pi/2} \sin\theta\,\mathrm{d}\theta \int_{p(-r,-h,\theta)-2t}^{p(r,h,\theta)} \mathrm{d}p \qquad (10)\\ &= \pi(2h + \pi r + 4t)\end{aligned}$$

Note 1. For $t = 0$, the last integral in Eq. 10 is equal to

$$p(r, h, \theta) - p(-r, -h, \theta) = H(\theta), \qquad (11)$$

namely the orthogonal projected length, or caliper length, of K onto an axis of direction (ϕ, θ), for any $\phi \in [0, 2\pi)$. Therefore, the mean caliper length with respect to the rotation invariant, (namely isotropic), probability element

$$\mathbb{P}(\mathrm{d}\phi,\ \mathrm{d}\theta) = \frac{\mathrm{d}\phi}{2\pi} \cdot \sin\theta\,\mathrm{d}\theta \qquad (12)$$

is,

$$\mathbb{E}\{H(\theta)\} = (2\pi)^{-1}\mu(h, r, 0) = h + (\pi/2)r \qquad (13)$$

Stereological references are for instance Fullman (1953), or Gundersen (1979). Recall that h is half the cylinder length.

HITTING PROBABILITIES

If $0 \leq t \leq h < \infty$ then, in order to compute μ_k, ($k = 0, 1, 2$) the limits of θ in the pertinent integral depend on an angle $\alpha := \alpha(h, r, t) \in [0, \pi/2]$, (Fig. 4a), such that, whenever $\theta \in [0, \alpha]$, the slab $L_t(p, \theta)$ cannot hit both bases of the cylinder, i.e., $\mu_2 = 0$.

Lemma 1. *For* $0 \leq t \leq h < \infty$ *and* $t \neq r$,

$$\tan\alpha = \frac{hr - t\sqrt{h^2 + r^2 - t^2}}{r^2 - t^2}. \qquad (14)$$

For $t = r$,

$$\tan\alpha = \frac{h^2 - r^2}{2hr}. \qquad (15)$$

If $0 \leq h \leq t < \infty$, *then* $\alpha = 0$.

Proof. With reference to Fig. 4a,

$$\tan\alpha = c/(2r), \quad \cos\alpha = 2t/(2h - c) \qquad (16)$$

Eliminating c, Eq. 14 is obtained. On the other hand, Eq. 15 is obtained by a passage to the limit as $t \to r$, applying for instance L'Hôpital's rule. Finally, if $t = h$ then Eq. 14 yields $\alpha = 0$ whereas, if $t > h$, then Eq, 14 is not defined and we may also set $\alpha = 0$.

Remark 1. Both the numerator and the denominator in the rhs of Eq. 14 are either positive, or negative, according to whether $t < r$, or $t > r$, respectively. Thus, $\tan\alpha > 0$.

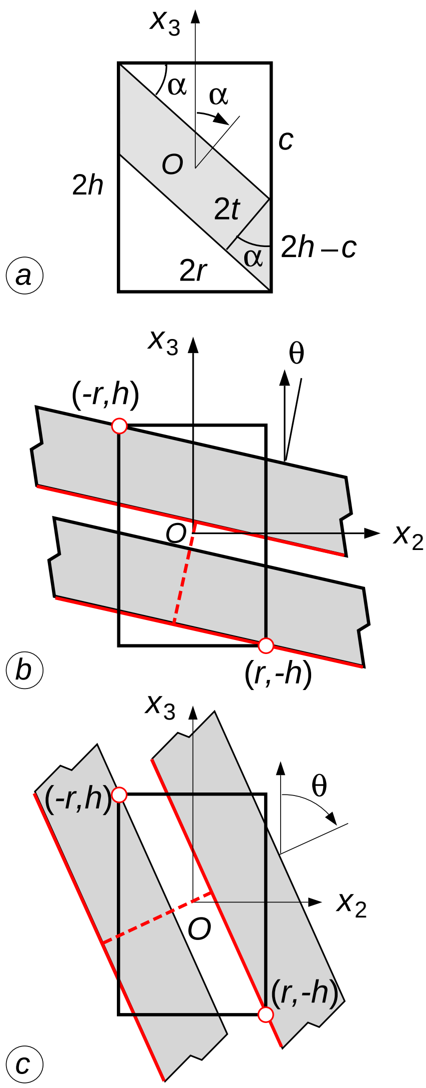

Fig. 4: *(a) Detail of the derivation of Eq. 14. (b) Idem of Eq. 19, when the slab does not hit any of the two cylinder bases. (c) Idem of Eq. 20, when the slab hits both cylinder bases.*

Proposition 1. *Consider the event $L_t \cap K \neq \emptyset$, where L_t is a 3D slab of thickness $2t$ equipped with the motion invariant density, and K is a fixed right circular cylinder of radius r and length $2h$. Conditional on the hitting event, the probabilities $P_k := P_k(h,r,t)$ defined in Eq. (6) read as follows.*

Case $0 \le t \le h < \infty$, with α given by Eq. 14 if $t \neq r$, and by Eq. 15 if $t = r$.

$$\begin{aligned}
P_0 &= \frac{r[-2\alpha + \sin(2\alpha)] - 4t(1-\cos\alpha) + 2h\sin^2\alpha}{2h + \pi r + 4t}, \\
P_1 &= \frac{r[4\alpha - 2\sin(2\alpha)] + 8t(1-\cos\alpha) + 4h\cos^2\alpha}{2h + \pi r + 4t}, \\
P_2 &= \frac{r[\pi - 2\alpha + \sin(2\alpha)] + 4t\cos\alpha - 2h\cos^2\alpha}{2h + \pi r + 4t}.
\end{aligned} \qquad (17)$$

Case $0 \le h \le t < \infty$. It suffices to set $\alpha = 0$ in the preceding expressions, namely,

$$\begin{aligned}
P_0(h,r,t) &= 0, \\
P_1(h,r,t) &= \frac{4h}{2h + \pi r + 4t}, \\
P_2(h,r,t) &= \frac{-2h + \pi r + 4t}{2h + \pi r + 4t}.
\end{aligned} \qquad (18)$$

Proofs. In the rhs of Eq. 7 the denominator is given by Eq. 10. Now, with reference to Fig. 4b,

$$\mu_0 = 2\pi \int_0^{\alpha} \sin\theta \mathrm{d}\theta \int_{p(r,-h,\theta)}^{p(-r,h,\theta)-2t} \mathrm{d}p \qquad (19)$$

which, recalling Eq. 9, yields π times the numerator of $P_0(h,r,t)$ in the first Eq. 17. Next, with reference to Fig. 4c,

$$\mu_2 = 2\pi \int_{\alpha}^{\pi/2} \sin\theta \, \mathrm{d}\theta \int_{p(-r,h,\theta)-2t}^{p(r,-h,\theta)} \mathrm{d}p \qquad (20)$$

yields π times the numerator of $P_2(h,r,t)$. Finally, because the hitting events $\{E_0, E_1, E_2\}$ are mutually exclusive,

$$P_1(h,r,t) = 1 - P_0(h,r,t) - P_2(h,r,t). \qquad (21)$$

As a cross check,

$$\begin{aligned}
\mu_1 &= 4\pi \int_0^{\alpha} \sin\theta \mathrm{d}\theta \int_{p(-r,-h,\theta)-2t}^{p(r,-h,\theta)} \mathrm{d}p \\
&+ 4\pi \int_{\alpha}^{\pi/2} \sin\theta \, \mathrm{d}\theta \int_{p(-r,-h,\theta)-2t}^{p(-r,h,\theta)-2t} \mathrm{d}p,
\end{aligned} \qquad (22)$$

yields π times the numerator of $P_1(h,r,t)$. The factor 4π instead of 2π stems because the latter factor would yield the hitting measure for only one of the two bases of the cylinder.

Corollary 1. *Let Y denote the spine of the cylinder K, that is the straight line segment*

$$Y := \left\{x \in \mathbb{R}^3 : x_1 = x_2 = 0, -h \le x_3 \le h\right\}, \qquad (23)$$

and define the conditional probability that the slab contains Y, namely,

$$P(h,r,t) = \mathbb{P}(L_t \supset Y \mid L_t \cap K \neq \emptyset). \quad (24)$$

If $0 \le t \le h < \infty$*, then,*

$$P(h,r,t) = \frac{2t^2/h}{2h+\pi r+4t}. \quad (25)$$

If $0 \le h \le t < \infty$*, then,*

$$P(h,r,t) = \frac{4t-2h}{2h+\pi r+4t}. \quad (26)$$

Proofs. The event $L_t \supset Y$ is equivalent to the event that L_t hits both endpoints of Y; moreover, Y may be regarded as a cylinder of length $2h$ and radius $r = 0$. In the first case, for $r = 0$ Eq. 14 yields $\alpha = \cos^{-1}(t/h)$, and making both substitutions in the numerator of the third Eq. 17, the numerator of Eq. 25 is obtained. For the second case, setting $r = 0$ in the numerator of the third Eq. 18, the numerator of Eq. 26 is obtained.

Corollary 2. *If the hitting probe is a plane* $L(p,\phi,\theta)$ *instead of a slab, namely if* $t = 0$*, then,*

$$\begin{aligned} P_0(h,r,0) &= \frac{2h-2r\tan^{-1}(h/r)}{2h+\pi r}, \\ P_1(h,r,0) &= \frac{4r\tan^{-1}(h/r)}{2h+\pi r}, \\ P_2(h,r,0) &= \frac{\pi r-2r\tan^{-1}(h/r)}{2h+\pi r}. \end{aligned} \quad (27)$$

Proofs. For $t = 0$, Eq. 14 yields $\alpha = \tan^{-1}(h/r)$, and making both substitutions in Eq. 17, Eq. 27 is obtained.

Note 2. In the preceding case, if $h = 0$, namely if K becomes a two sided disk of finite radius r and perimeter length B, then,

$$\begin{aligned} P_0(0,r,0) &= P_1(0,r,0) = 0 \\ P_2(0,r,0) &= 1 \end{aligned} \quad (28)$$

Here $\mu_2(0,r,0) = \mu(0,r,0) = \pi^2 r$, a well known result, see e.g. Cruz-Orive (2024), Eq. 1.19.21 with $B = 2\pi r$.

APPLICATION TO THE WEIBEL-PALADE BODIES

The numerical results in this section correspond to a WP body modelled by a right circular cylinder of radius $r = 0.035\,\mu$m and half length $h = 0.500\,\mu$m. The results are intended to be only orientative. Probabilities will be rounded to third significant digit.

OBSERVATION PROBABILITIES WITH PLANAR SECTIONS

This model assumes that TEM sections are stained on its upper face, whereby a WP body transect would be equivalent to a planar transect. The application of the third Eq. 27 yields,

$$P_2(0.500, 0.035, 0) = 0.00441 \quad (29)$$

which means that the expected proportion of 'longitudinal' transects among all possible IUR transects would be of 4.4 in a thousand.

In a population of n IUR planar transects, let n_2 denote the random number of 'longitudinal' transects. Under suitable independence assumptions, the distribution of n_2 may be approximated by the Poisson distribution of mean nP_2, whereby,

$$\begin{aligned} \mathbb{P}(n_2 \ge 1) &= 1 - \mathbb{P}(n_2 = 0) \\ &= 1 - \exp(-nP_2). \end{aligned} \quad (30)$$

For instance, among $n = 30$ IUR transects, the probability of obtaining at least one 'longitudinal' transect would be,

$$\begin{aligned} \mathbb{P}(n_2 \ge 1) &= 1 - \exp(-30 \cdot 0.00441) \\ &= 0.124 \end{aligned} \quad (31)$$

that is, the probability of obtaining none would be of about 88%.

OBSERVATION PROBABILITIES WITH SLAB SECTIONS

This model may be less realistic inasmuch as ultrathin TEM slices of biological material are usually not transparent.

Adopt a half section thickness $t = 0.030\,\mu$m. Then, applying Eq. 14,

$$\alpha(0.500, 0.035, 0.030) = 1.441\,\text{rad}, \quad (32)$$

namely about 82.6°. Now the third Eq. 17 yields the probability that the slab hits both bases of the cylinder, conditional to the event that the slab hits the cylinder. Thus,

$$P_2(0.500, 0.035, 0.030) = 0.0137, \quad (33)$$

which means that the expected proportion of transects involving both ends of the cylinder model (or 'longitudinal' transects, for short) would be of 1.37%

among all possible IUR transects. Now, among $n = 30$ IUR transects,

$$\mathbb{P}(n_2 \geq 1) = 1 - \exp(-30 \cdot 0.0137) \qquad (34)$$
$$= 0.337$$

which means that the probability of obtaining none would now be of about 66%.

Finally, the conditional probability that the slab contains the spine of the cylinder is given by Eq. 25, which yields,

$$P_2(0.500, 0.035, 0.030) = 0.00293. \qquad (35)$$

Under this model, the probability of obtaining at least a 'longitudinal' transect among $n = 30$ IUR transects is,

$$\mathbb{P}(n_2 \geq 1) = 1 - \exp(-30 \cdot 0.00293) \qquad (36)$$
$$= 0.0841$$

i.e., the probability of obtaining none would now be of about 92%. Under this model the identification of 'longitudinal' transects may be easier than under the planar sections one, inasmuch as grazing sections of the cylinder bases would be nearly absent.

CLOSING COMMENTS

Under the cylinder model, the probability that an IUR planar transect of a WP body of $1.00\,\mu$m length and $0.07\,\mu$m diameter affects both ends of the body - namely the probability that the transect is 'longitudinal', is about 4 in a thousand, (Eq. 29). On the other hand, the corresponding probability that the transect contains the spine of the cylinder is still less, namely about 3 in a thousand, (Eq. 35). This tends to agree with Ewald Weibel's guess that the mentioned probability "is extremely low". (The adopted WP body size is suggested by the longitudinal transect marked with two red arrows in Fig. 2).

With the preceding data, if the total number of WP body transects in a section image analogous to Fig. 2 was 30, say, (i.e., about 2× the number of white arrows, as suggested personally by E.R. Weibel) then the a priori probability of obtaining at least one longitudinal transect might lie between 1 in 8, (Eq. 31), and 1 in 12, (Eq. 36) - we may leave it in 1 in 10, say. However, the a priori probability of not only observing it, but also realising that the longitudinal transect marked in red in Fig. 2 corresponded to a new organelle, and not to an artifact, might have been rather less than 1 in 10. This is analogous to spotting a winning chess combination without being told that there is "something" there.

With regard to the estimation of the total number N of WP bodies in a well defined 3D compartment, the application of the physical disector (Sterio, 1984) on TEM sections may be inefficient, mainly because the unambiguous identification of a WP body transect depends on the outcome of a rare event (E_2, see Eq. 5). The optical disector, which is based on a sweeping optical section, (Gundersen, 1986, West et al., 1996), aided by immunofluorescence imaging (e.g. Valentijn *et al.*., 2011), or similar techniques, could be a choice but, to our knowledge, no results have hitherto appeared in the literature. At least as important as number may be total volume, V, say. Its design unbiased estimation, however, requires sections of "zero thickness". This may be feasible if only the upper face of a slice is stained but then, a more severe requirement is that every WP transect present in a section (not only the longitudinal ones) should be unambiguously identified. More simply, if N was available, and if the WP bodies were approximately rods of a nearly constant volume v, then, tentatively $V = v \cdot N$.

Among other authors, Valentijn *et al.*. (2011) show that WP bodies are often twisted, and even coalescent with one another - the rod model adopted here was intended mainly as a tribute to Ewald Weibel's discovery.

Note 3. This paper was submitted for publication to IAS on 5 May 2026. Around that time, the media reported a Hantavirus outbreak aboard the cruise ship MV Hondius. In humans, Hantavirus Pulmonary Syndrome (HPS) triggers the exocytosis of Weibel-Palade bodies, thereby releasing von Willebrand factor into the bloodstream. As a consequence, the pulmonary capillaries become permeable, potentially leading to pulmonary edema (lung flooding).

ACKNOWLEDGMENT

The author shared a few E-mails with Ewald Weibel over 2012-2013, on the occasion of the 50th anniversary of his discovery. He provided details and insights used in this note, as well as Figs. 1 and 2, and reprints (Weibel, 2012a, b).

REFERENCES

Cruz-Orive LM (2017). Stereology: a historical survey. Image Anal Stereol 36:153-177.

Cruz-Orive LM (2024). Stereology. Theory and Applications. Interdisciplinary Applied Mathematics 59. Cham: Springer Nature Switzerland AG.

Fullman RL (1953) Measurement of approximately cylindrical particles in opaque samples. J Metals/AIME Trans 197:1267-1268.

Gundersen HJG (1979). Estimation of tubule or cylinder L_V, S_V, and V_V on thick sections. J Microsc 117:333-45.

Gundersen HJG (1986). Stereology of arbitrary particles. A review of unbiased number and size estimators and the presentation of sorne new ones, in memory of William R. Thompson J Microsc 143:3-45.

Miles RE, Davy PJ (1976). Precise and general conditions for the validity of a comprehensive set of stereological fundamental formulae. J Microsc 107:211-226.

Naveira AM, Reventós A, eds. (2009). Luis Antonio Santaló. Selected Works. Berlin: Springer.

Santaló LA (1936). Geometría integral 7: Nuevas aplicaciones del concepto de medida cinemática en el plano y en el espacio. Tesis doctoral. Rev Acad Ci Madrid 33:451-504. [Reprinted in Naveira AM, Reventós A, eds. (2009), pp. 167-212.]

Sterio DC (1984). The unbiased estimation of number and sizes of arbitrary particles using the disector. J Microsc 134:127-36.

Valentijn KM, Sadler JE, Valentijn JA, Voorberg J, Eikenboom J (2011) Functional architecture of Weibel-Palade bodies. Blood 117:5033-5043.

Weibel ER (2012a) Ewald Weibel: An organelle of his very own, and more. People & Ideas, J Cell Biol 197:4-5.

Weibel ER (2012b) Fifty years of Weibel-Palade bodies: the discovery and early history of an enigmatic organelle of endothelial cells. J Thromb Haemost 10:979-984.

Weibel ER, Palade GE (1964) New cytoplasmic components in arterial endothelia. J Cell Biol 23:101-112.

West MJ, Østergaard K, Andreassen OA, Finsen B (1996) Estimation of the number of somatostatin neurons in the striatum: An in situ hybridization study using the optical fractionator. J Comp Neurol 370:11-22.